

Published in final edited form as:

Hepatology. 2010 October ; 52(4): 1420–1430. doi:10.1002/hep.23804.

Role and Cellular Source of Nicotinamide Adenine Dinucleotide Phosphate Oxidase in Hepatic Fibrosis

Samuele De Minicis^{1,2}, Ekihiro Seki¹, Yong-Han Paik^{1,3}, Christoph H. Österreicher¹, Yuzo Kodama¹, Johannes Kluwe⁴, Luciano Torozzi², Katsumi Miyai⁵, Antonio Benedetti², Robert F. Schwabe⁴, and David A. Brenner¹

Samuele De Minicis: s_deminicis@libero.it; Ekihiro Seki: ekseki@ucsd.edu; Yong-Han Paik: ypaik@ucsd.edu; Christoph H. Österreicher: coesterr@ucsd.edu; Yuzo Kodama: ykodama@ucsd.edu; Johannes Kluwe: jk2693@columbia.edu; Luciano Torozzi: l.trozzii@univpm.it; Katsumi Miyai: kmiyai@ucsd.edu; Antonio Benedetti: a.benedetti@ospedaleiruniti.marche.it; Robert F. Schwabe: rfs2102@columbia.edu; David A. Brenner: dbrenner@ucsd.edu

¹ Department of Medicine, University of California San Diego, School of Medicine, California

² Gastrointestinal Unit, University of Ancona, Italy

³ Department of Internal Medicine, Yonsei University College of Medicine, Seoul, Korea

⁴ Department of Medicine, Columbia University, New York

⁵ Department of Pathology, University of California San Diego, School of Medicine, California

Abstract

Reactive oxygen species (ROS) generated by Nicotinamide adenine dinucleotide phosphate oxidase (NOX) is required for liver fibrosis. This study investigates role of NOX in ROS production and the differential contribution of NOX from bone marrow (BM) derived and non-BM derived liver cells. Hepatic fibrosis was induced by bile duct ligation (BDL) for 21 days or by methionine-choline deficient (MCD) diet for 10 weeks in wild-type (WT) mice and mice deficient in p47phox (p47phox KO), a component of NOX. p47phox KO chimeric mice were generated by the combination of liposomal clodronate injection, irradiation and BM transplantation of p47phox KO BM into WT recipients and vice versa. Upon BDL, chimeric mice with p47phox KO BM-derived cells, including Kupffer cells (KC), and WT endogenous liver cells showed a ~25% reduction of fibrosis, while chimeric mice with WT BM-derived cells and p47phox KO endogenous liver cells, including hepatic stellate cells (HSC), showed a ~60% reduction of fibrosis. In addition, p47phox KO compared to WT mice treated with an MCD-diet showed no significant changes in steatosis and hepatocellular injury, but a ~50% reduction in fibrosis. Cultured WT and p47phox KO HEP treated with free fatty acids (FFA) had a similar increase in lipid accumulation. FFA promoted a 1.5 fold increase in ROS production both in p47phox KO and in WT hepatocytes (HEP).

Conclusion—NOX in both BM derived and non-BM derived cells contributes to liver fibrosis. NOX does not play a role in experimental steatosis and the generation of ROS in HEP, but exerts a key role in fibrosis.

Correspondence should be addressed to: David A. Brenner M.D., University of California San Diego, School of Medicine, Vice Chancellor Health Sciences Office, 9500 Gilman Drive #0602, La Jolla, CA 92093-0602, Phone: 858-534-1501, Fax: 858-822-0084, dbrenner@ucsd.edu.

No conflicts of interest exist.

Keywords

hepatic stellate cells; reactive oxygen species; fibrogenesis; bone marrow transplantation; methionine and choline deficient diet

INTRODUCTION

Liver fibrosis is the consequence of chronic liver injury and represents an important cause of mortality worldwide (1,2). Liver fibrosis results from inflammation associated with the production of chemokines and cytokines that stimulate and act on different cells in the liver, including hepatic stellate cells (HSC), Kupffer cells (KC), hepatocytes (HEP), and endothelial cells (3,4). The endpoint of advanced liver fibrosis is cirrhosis, in which the fibrous scar and regenerating nodules lead to hepatocellular dysfunction, portal hypertension, and hepatocellular carcinoma (5,6). An inflammation-fibrosis-cancer axis has therefore been proposed (7). Oxidative stress plays an important role in inflammation, fibrosis, and cancer (8–10). Nicotinamide adenine dinucleotide phosphate (NADPH) oxidase (NOX), a key source of reactive oxygen species (ROS) in the liver (11), may therefore represent an important new therapeutic target (12). NOX is a multiprotein complex that catalyzes ROS formation in response to many stimuli (9,13). Macrophages, including KC, express the phagocytic form of NOX that plays a crucial role in antimicrobial defence (8,14–16). The non-phagocytic form of NOX is expressed in other cell types, such as vascular smooth muscle cells and cardiac myofibroblasts, and is required for the proper activation of many intracellular signalling pathways, including mitogen-activated protein kinase (MAPK) and PI3K (11,17,18). We have previously shown that NOX is required for hepatic fibrosis in vivo (9). KC express the majority of NOX in the liver and play an important role in HSC activation (19). However, NOX is also expressed by HSC and is able to mediate hepatic stellate cell activation in response to fibrogenic agonists such as platelet-derived growth factor (PDGF), angiotensin II (Ang II) and leptin (9,18,20). Furthermore, HEP contain NOX (21), providing a potentially additional sources of ROS in inflammation and fibrosis. However, the relative contribution of NOX in KC, HEP and HSC to hepatic inflammation and fibrosis remains unknown. This study demonstrates that NOX-mediated formation of ROS in non-BM derived liver cells play a key role in liver fibrosis.

MATERIAL AND METHODS

Chemicals

2',7'-Dichlorofluorescein diacetate (CM-H₂ DCFDA) was purchased from Molecular Probe Inc. (Eugene, OR). Palmitic acid was purchased from Sigma Aldrich (St. Louis, MO).

Animal and treatment

p47^{phox}-deficient mice on a C57BL/6 background, which lack a critical cytosolic component required for assembly of an active NADPH oxidase complex, and p47^{phox}-sufficient wild-type (WT) C57BL/6 control mice were purchased from Taconic Corp. (Hudson, NY) (22). Six to eight week-old male mice were used for liver injury experiments and for diet treatment. Liver fibrosis was induced either by bile duct ligation (BDL) or by intra-peritoneal injection of the hepatotoxin carbon tetrachloride (CCl₄). Mice were housed in a pathogen-free barrier facility accredited by the Association for the Accreditation and Assessment of Laboratory Animal Care.

Diet treatment

Mice were fed ad libitum a high-fat, methionine and choline-deficient (MCD) diet (ICN Biomedicals, Sydney, Australia) for up to 10 weeks (23). Controls were pair-fed the same diet supplemented with choline chloride (2 g/kg) and DL-methionine (3 g/kg) (MCS diet).

Cell culture

Mouse HEP were isolated from WT and P47phox-deficient mice as described previously (9,11). HEP were subsequently plated on dishes coated with type I collagen and cultured in Waymouth's medium (GIBCO BRL; Life Technologies) containing 10% fetal bovine serum, 0.1 mmol/l insulin, and 0.1 mmol/l dexamethasone. After 2 hours, the cultures were washed with phosphate buffered saline and changed to RPMI medium (GIBCO BRL). HEP were incubated with agonists for an additional 12 hours (24). HEP, KC, endothelial cells, fibrocytes and HSC were isolated from control and BDL mice, as previously described (9,25,26).

Histochemical studies

Paraffin-embedded sections were stained with H&E and Sirius red. For immunohistochemical analysis, sections were deparaffinized, rehydrated, and stained using the DAKO EnVision system protocol (DAKO, Carpinteria, CA). Sections were incubated with anti alpha-Smooth Muscle Actin (α -SMA) (1:1,000; DAKO) or 4-hydroxynonenal (4-HNE) for 30 minutes at room temperature. As negative controls, all specimens were incubated with an isotype-matched control antibody. The area of positive staining was measured using a computer-based morphometric analysis system. For immunofluorescence analysis, frozen sections were incubated with antibodies for 4-HNE, α -SMA (DAKO), F4/80 (eBioscience) or pan-cytokeratin (Biolegend) overnight.

Quantification of hepatic collagen content

Collagen content was assessed by both morphometric analysis of Sirius red staining of liver sections and by hydroxyproline concentration. The area of positive Sirius red staining was measured using a computerized analysis method. Hydroxyproline content was quantified colorimetrically from 0.1 g liver samples.

Measurement of intracellular ROS

Cells cultured in 24-well plates were loaded with the redox-sensitive dye DCFDA (10 μ M) for 20 minutes at 37°C. Cells were then stimulated with an agonist. DCFDA fluorescence was detected at excitation and emission wavelengths of 488 nm and 520 nm, respectively (9). ROS formation was measured using a multiwell fluorescence scanner (CytoFluor 2300; Millipore, Bedford, MA).

Western blotting

Liver extracts were obtained in a modified radioimmunoprecipitation buffer as described previously (18). Western blotting was performed using standard protocols. An antibody against α -SMA (Sigma-Aldrich) was used at the concentration of 1:1000. Horseradish peroxidases-conjugated secondary antibodies were used and visualized using enhanced chemiluminescence.

Bone marrow transplantation

Bone marrow transplantation (BMT) was performed as described previously (25). Mice received an intravenous injection of liposomal clodronate (200 μ l intravenously) before irradiation to deplete KC (27). Tibias and femurs of donor mice were flushed to obtain bone

marrow (BM). 1×10^7 BM cells were injected into the tail veins of lethally irradiated (11 Gy) recipient mice. BDL was performed 12 weeks after BMT. To determine successful BMT in p47phox-deficient and p47phox-sufficient mice, spleen cells were isolated from BDL chimeric mice and analyzed by quantitative real-time polymerase chain reaction (RT-PCR) to measure p47phox mRNA expression (data not shown).

Quantitative real-time PCR

RT-PCR was used for measuring mRNA levels of fibrogenic markers (Collagen $\alpha 1(I)$ and α SMA). Extraction of RNA from total liver mice was performed by a combination of TRIzol (Invitrogen, Carlsbad, CA) and RNeasy columns (Qiagen, Valencia, CA). cDNA was obtained using the Amersham kit for cDNA synthesis (11).

Statistical analysis

Results are expressed as mean \pm SEM. The results were analyzed using the unpaired Student's t test or the Newman-Keuls test. A p value of less than 0.05 was considered statistically significant.

RESULTS

p47phox-deficient mice are resistant to liver fibrosis induced by BDL or CCl₄

To assess the role of the NOX in liver fibrosis, p47phox knock out (KO) mice were subjected to two different models of hepatic damage: BDL as a model of cholestatic liver injury and CCl₄ treatment as a model of toxic liver injury. Consistent with our previous studies (9), mice deficient for the p47phox component of NOX had reduced fibrosis after three weeks of BDL, as evaluated by collagen deposition and α -SMA staining (Fig. 1A, B). Furthermore, the critical role of NOX in liver fibrosis was confirmed in mice subjected to intra-peritoneal injection of CCl₄. Mice received 16 injections of CCl₄ (0.5 μ L/g; twice weekly) and were sacrificed two days after the last injection. WT mice displayed a significant increase in collagen deposition and α -SMA staining following treatment with CCl₄ compared to vehicle treated mice (Fig. 1C, D). The increase in fibrotic parameters was significantly reduced in p47phox-deficient mice (Fig. 1C, D). In addition, mRNA levels of collagen $\alpha 1(I)$ and α -SMA were significantly reduced in p47phox-deficient mice compared to p47phox-sufficient mice either after three weeks of BDL or after 16 injections of CCl₄ as evaluated by RT-PCR (Fig. 1E, F). Moreover, the protein expression of α -SMA was reduced in p47phox-deficient mice in comparison to p47phox-sufficient mice, either after BDL or CCl₄ (Fig. 1E, F). These data demonstrate that NOX plays a crucial role in the pathogenesis of liver fibrosis in two complimentary models of liver injury.

NOX in hepatic stellate cells plays a crucial role in cholestatic liver injury

To investigate the expression of NOX in different cell population of the liver, we performed RT PCR for the mRNA levels of the main components of NOX activity in different cells of the liver: fibrocytes, KC, HEP, endothelial cells and HSC. The data showed that the p47phox component is mainly expressed in KC, among the BM-derived cells, and in HSC, among the non-BM-derived cells (Fig. 2A). Surprisingly, HEP expressed p47phox. Furthermore, the data showed a lower expression of this component in other cell types of the liver (Fig. 2A). Concordantly with the p47phox mRNA expression in the different hepatic cell types, we performed double immunofluorescence staining between 4-HNE (a lipid peroxidation product as a general marker of ROS) and cell type markers F4/80, α SMA and pan-cytokeratin for KC, HSC and parenchymal cells, respectively. 4-HNE was expressed in KC and HSC in the livers of BDL mice (Fig. 2B,C). Some HEP also express ROS in BDL

mice (Fig. 2D). We further confirmed that these cell types express ROS in the livers of CCl₄-treated mice (Sup Fig. 1).

To investigate the role of NOX from different hepatic cell types in liver fibrosis, BMT was employed to generate chimeric mice. BM from p47phox-sufficient mice was transplanted into p47phox-deficient mice and vice versa, obtaining mice with NOX-sufficient BM-derived cells, including KC and NOX-deficient endogenous liver cells (non-BM derived), including HSC, and vice versa. As controls, BM from p47phox-deficient mice was transplanted into p47phox-deficient mice and BM from p47phox-sufficient mice was transplanted into p47phox-sufficient mice. This strategy produced 4 different groups of mice: 1) WT BM → p47phox KO mice, 2) WT BM → WT mice, 3) p47phox KO BM → WT mice, 4) p47phox KO BM → p47phox KO mice. We have previously shown that this strategy is useful in discriminating signalling pathways between HSC and KC (25). In summary, this resulted in mice with HSC deficiency for p47phox but with normal KC (group 1), mice with intact NOX in all cells (group 2), mice with NOX-deficient KC but WT HSC (group 3), and mice deficient for NOX in all cells (group 4). These mice were then subjected to BDL for 3 weeks.

As expected from our above results, mice with intact NOX (group 2) showed the most fibrosis and mice deficient for p47phox in all cells (KO → KO, group 4) showed the least fibrosis (Fig. 3A–C). Deficiency for p47phox in either BM derived or non-BM derived cells resulted in attenuated liver fibrosis following 3 weeks of BDL as evaluated by collagen deposition and hydroxyproline content compared to mice with functional p47phox in all cells (WT BM → WT mice, group 2) (Fig. 3A–C). Furthermore, chimeric mice with NOX-deficient endogenous liver cells, including HSC, but WT BM derived cells, including KC, (WT BM → p47phox KO mice, group 1), showed reduced levels of collagen deposition and hydroxyproline content in comparison to chimeric mice with NOX-sufficient endogenous liver cells, including HSC, but NOX-deficient BM derived cells (p47phox KO BM → WT mice, group 3) (Fig. 3A–C). Accordingly, chimeric mice with NOX-deficient endogenous liver cells but WT BM derived cells showed a significant reduction of α -SMA expression, as demonstrated by immunohistochemistry and western blotting (Fig. 3D, E). Moreover, mRNA expression for α -SMA and collagen α 1(I) confirmed the reduced expression of fibrogenic markers in chimeric mice with NOX-deficient HSC (Fig. 3F). These results suggest that NOX-mediated generation of ROS in endogenous liver cells, including HSC, is more important than in BM derived cells, including KC, for the development of fibrosis following cholestatic liver injury.

Chimeric mice with NOX-deficient endogenous liver cells showed reduced peroxidation

NOX generates ROS in many cell types. To investigate the levels of peroxidation in the NOX-chimeric livers, mice subjected to BMT were analyzed for peroxidation by immunohistochemistry for hydroxynonenal adducts. As expected, NOX-deficient mice showed reduced peroxidation in comparison to NOX-sufficient mice. Interestingly, chimeric mice with NOX-deficient HSC showed a reduced level of peroxidation, confirming the importance of oxidative stress produced by NOX in HSC during the process of liver fibrosis. (Fig. 4A).

Peroxidation was also measured in whole liver samples by thiobarbituric acid reactive substances (TBARS) assays. Peroxidation in chimeric livers with NOX-deficient hepatic stellate cells had a greater reduction in lipid peroxidation than the chimeric livers with NOX-deficient KC. In fact, the level of peroxidation produced by these chimeric mice was similar to the peroxidation in complete p47phox KO mice (Fig. 4B).

To better differentiate the ROS activity in the different cell type in the liver, we performed double immunofluorescence for 4-HNE and α SMA in the chimeric mice (Fig. 4C, D). The experiment showed a co-localization of ROS production (HNE stain) and HSC in chimeric mice with p47phox KO BM (p47phox KO BM \rightarrow WT mice) subjected to BDL (Fig. 4C), while HSC express little ROS in the chimeric mice with p47phox KO endogenous liver cells (WT BM \rightarrow p47phox KO mice) subjected to BDL (Fig. 4D), suggesting that NOX is a major contributor in HSC.

MCD diet induces hepatic steatosis independent of NADPH oxidase

To investigate the role NOX in a mouse model of non-alcoholic steatohepatitis (NASH) ultimately leading to fibrosis, NOX-deficient (p47phox KO) mice and WT controls were fed an MCD diet for 10 weeks. Although both WT and KO mice fed the MCD diet lost weight, the liver weight-body weight fraction revealed an increase in steatosis of the liver of all MCD-treated mice (Fig. 5A). In addition, the serum transaminases levels were significantly higher both in WT and KO mice fed the MCD diet than the MCS diet (Fig. 5B), suggesting an equal degree of steatosis and of hepatocellular damage both in WT and in KO mice. To confirm these results, RT-PCR for the mRNA of inflammatory markers such as MCP-1 and TNF α showed no significant differences in WT and KO mice fed the MCD diet (Fig. 5C). However, there was significant difference in the mRNA expression of TIMP-1, a marker of HSC activation (Fig. 5C).

Livers from mice fed an MCD diet showed significant deposition of triglycerides, with macro- and micro-nodular distribution of fat as evaluated by Oil-red O staining compared to mice fed a control diet supplemented with methionine and choline (Fig. 5D, E). The higher deposition of fat in mice fed the MCD diet was confirmed by measuring hepatic triglycerides content (Fig. 5F). A slight increase in fat deposition in mice receiving the MCS control diet was observed compared to mice fed a normal chow diet (Fig. 5D, E). There was no difference in hepatic lipid content between NOX-deficient and WT mice (Fig. 5D–F). This suggests that NOX is dispensable for fat accumulation in a mouse model of non-alcoholic fatty liver disease (NAFLD).

MCD diet induces similar levels of peroxidation in the livers of WT and NOX-deficient mice

Oxidative stress is a hallmark of NASH, which is recapitulated in mice fed an MCD diet. Reductions in antioxidant defence mechanisms as well as increases in ROS production are attributed to methionine-choline deficiency. Immunohistochemistry for 4-HNE adducts showed similar staining in the livers of NOX-deficient (p47phox KO) and WT mice fed an MCD diet, indicating a diet induced increase in ROS production that is independent of NOX (Fig. 6A). Accordingly, TBARS levels were significantly increased in mice fed an MCD diet compared to MCS diet, but no difference between WT and KO mice was observed (Fig. 6B). This result was confirmed by immunofluorescence staining in MCS and MCD fed mice that revealed 4-HNE in the hepatocytes of both WT and KO MCD fed mice (Fig. 6C). Thus, the generation of total hepatic ROS in this NASH model is independent of NOX.

NOX is critical for the development of MCD diet induced liver fibrosis

Even if NOX does not affect fat accumulation and generation of total hepatic ROS, it might still affect the development of liver fibrosis following an MCD diet. Sirius red staining indicated that feeding an MCD diet for 10 weeks results in significant fibrosis in WT mice compared to mice fed an MCS diet. However, NOX-deficient (p47phox KO) mice fed an MCD diet failed to develop fibrosis (Fig. 7A). Collagen α 1(I) and α -SMA mRNAs were increased in WT mice fed an MCD diet in comparison to mice fed the control MCS diet. This increase in fibrogenic markers was significantly attenuated in NOX-deficient mice fed an MCD diet (Fig. 7B). Collectively, these data suggest that NOX is not involved in lipid

metabolism and hepatic fat accumulation but NOX is required for the development of fibrosis in the metabolic model of liver disease. Indeed, HSC express ROS in WT, but not NOX-deficient, mice fed an MCD diet (Sup Fig. 2)

FFA-induced ROS production in HEP is NOX-independent

Our data suggest that the MCD diet causes steatosis and oxidative stress independent of NOX, but that the subsequent development of fibrosis in this model of metabolic liver injury relies on NOX. To further evaluate the role of NOX in HEP, we isolated primary HEP from NOX-deficient (p47phox KO) and WT mice and incubated them with palmitic acid (200 μ M) for 12 hours. Oil-red O staining showed a similar extent of triglyceride accumulation in WT and NOX-deficient HEP (Fig. 8A). Moreover, incubation with palmitic acid caused a significant increase in ROS production as evaluated by DCFDA measurement in comparison to untreated cells (Fig. 8B). However, increases in ROS production were similar between WT and p47phox-deficient HEP (Fig. 8B). Thus, NOX is not required for FFA-induced triglyceride accumulation and ROS generation in HEP.

DISCUSSION

NOX is a multi-protein complex that generates ROS in response to a wide range of stimuli (28). In the liver, NOX is expressed in both phagocytic and non-phagocytic forms. Chronic liver diseases are characterized by increased ROS production as well as decreased activity of antioxidant systems, resulting in oxidative stress (29). This feature is commonly detected in patients with alcoholic liver disease, hepatitis C virus infection, hemochromatosis, and cholestatic liver diseases. Similar observations were made in experimental models of liver fibrosis. Oxidative stress is not only a consequence of chronic liver injury but also significantly contributes to excessive tissue remodelling and fibrogenesis (30). NOX has emerged as a primary source of ROS in liver disease. KC in the liver mainly produces ROS through the phagocytic form of NOX (16), which exerts an important role in host defence and inflammation (31). HSC express a non-phagocytic form of NOX, which plays a critical role in activating signalling pathways (9,32). Fibrogenic agonists such as Ang II, leptin, PDGF, and apoptotic bodies activate NOX in cultured HSC (9,17,18,20,33). Both pharmacological inhibition with diphenyleneiodonium (DPI) (34) and genetic studies using p47phox-deficient mice provided evidence for a central role of NOX in the regulation of HSC activation and liver fibrosis. Whereas there is convincing data regarding the in vitro activation of HSC (35), the contribution of NOX in different hepatic cell types to hepatic fibrogenesis in vivo remains mostly unknown. Since KC are the major source of phagocytic NOX in the liver and are required for HSC activation and fibrogenesis (36), it could be possible that phagocytic NOX is the main mediator of hepatic fibrogenesis (37), or that both KC and HSC mediate fibrogenesis. Our study used BMT to compare the contribution of NOX-derived ROS from BM-derived cells, including KC, and endogenous liver cells, including HSC, to hepatic fibrosis. Our data show that NOX in both BM-derived cells and endogenous liver cells contributes to liver fibrogenesis.

Earlier studies proposed that the NOX in Kupffer cells was critical for alcoholic liver disease (38). However, this model produced steatosis and inflammation, but not fibrosis. In fact, the current study demonstrated that chimeric mice with NOX-deficient HSC but WT KC had the greatest reduction in liver fibrosis. The possibility of creating a selective inhibition of the non-phagocytic form of NOX (39–41) without the involvement of the phagocytic form should significantly reduce the fibrogenic pathway without affecting host defence mechanisms related to the functionality of the phagocytic form of NOX (42).

NAFLD, the liver manifestation of the metabolic syndrome, may progress to liver fibrosis and cirrhosis(43). Moreover, while the main source of ROS production in both viral and

ethanol appears to result from activation of NOX (44–46), the role of NOX in NAFLD is still unclear. In fact, the main cell types involved in ROS production during NAFLD are perhaps HEP (47). HEP express a functional form of NOX that participates in CD95-induced cell death (21). Our study demonstrates that the development of steatosis, lipid peroxidation and inflammation caused by an MCD diet are independent from the p47 subunit of the NOX. This conclusion was supported by data showing the same triglyceride accumulation and ROS in primary cultures of HEP isolated from p47phox KO and WT mice. In fact, the majority of ROS production in MCD-induced liver injury is derived from hepatocellular lipid deposition and subsequent peroxidation. Other sources of ROS in HEP are the cytochrome P450s and mitochondrial respiratory chain (48,49).

However, our study revealed that NOX does play a role in the steatosis-inflammation-fibrosis axis in NAFLD, in that NOX-deficient mice express little ROS in HSC, and develop less fibrosis compared to WT mice on an MCD diet for 10 weeks (Fig. 7, Sup Fig. 2). Thus, NOX was required for ROS generation in HSC and fibrosis but not steatosis or ROS generation in HEP in this model of NAFLD. However, because the MCD diet is not as robust in inducing liver fibrosis as BDL or CCl₄, we could not perform the same chimeric liver studies to further identify the key cell types expressing NOX in the NASH model.

Another mechanism of fibrogenesis is represented by apoptosis and then phagocytosis of apoptotic bodies (33). Apoptotic bodies may directly or indirectly, through KC, activate HSC and promote myofibroblastic transdifferentiation. NOX plays a critical role in the process of phagocytosis in response to apoptotic bodies that are generated during liver injury. Thus, the reduced fibrosis observed in p47 KO mice may be related to the inhibition of the fibrogenic mechanism induced by apoptotic bodies.

In conclusion, our study points to a crucial role of non-phagocytic NOX in liver fibrosis but not steatosis in experimental liver fibrosis including NAFLD. Thus, not all ROS is the same, so that ROS generated by NOX in HSCs in fibrogenic, while ROS generated in steatotic hepatocytes is NOX-independent. Specific inhibition of non-phagocytic NOX components may inhibit fibrosis without interfering with the immune host defences, and thus represent a promising pharmacological target.

Supplementary Material

Refer to Web version on PubMed Central for supplementary material.

Acknowledgments

Grant support: This study was supported by a grant from an Alimenti e Salute grant from the University of Ancona and the American Liver Foundation Postdoctoral Fellowship (to S.D.M.), the American Association for the Study of Liver Diseases/American Liver Foundation Liver Scholar Award (to E.S.), the Austrian Science Fund Research Fellowship, American Gastroenterology Association Fellowship-to Faculty Transition Award (to C.H.Ö), the MIUR grant 2007 (prot. 2007HPT7BA_002) (to A.B.) and NIH R01DK072237 (to D.A.B.).

List of Abbreviations

Ang II	angiotensin II
α-SMA	alpha-Smooth Muscle Actin
BDL	bile duct ligation
BM	bone marrow
BMT	bone marrow transplantation

CCl₄	carbon tetrachloride
CM-H2 DCFDA	2',7'-Dichlorofluorescein diacetate
DPI	diphenyleneiodonium
FFA	free fatty acids
HEP	hepatocytes
4-HNE	4-hydroxynonenal
HSC	hepatic stellate cells
KC	Kupffer cells
KO	knock out
MAPK	mitogen-activated protein kinase
MCD	methionine-choline deficient
MCS	methionine-choline-sufficient
NADPH	Nicotinamide adenine dinucleotide phosphate
NAFLD	non-alcoholic fatty liver disease
NASH	non-alcoholic steatohepatitis
NOX	NADPH oxidase
PDGF	platelet-derived growth factor
ROS	reactive oxygen species
RT-PCR	quantitative real-time polymerase chain reaction
TBARS	thiobarbituric acid reactive substances
WT	wild-type

References

1. Bataller R, Sancho-Bru P, Ginès P, Brenner DA. Liver Fibrogenesis: a new role for the renin-angiotensin system. *Antioxid Redox Signal*. 2005 Sep–Oct 7.(9–10):1346–1355. Review. [PubMed: 16115040]
2. Friedman SL. Liver fibrosis -- from bench to bedside. *J Hepatol*. 2003; 38 (Suppl 1):S38–53. [PubMed: 12591185]
3. Kisseleva T, Brenner DA. Mechanisms of fibrogenesis. *Exp Biol Med (Maywood)*. 2008; 233:109–122. [PubMed: 18222966]
4. Kisseleva T, Brenner DA. Fibrogenesis of parenchymal organs. *Proc Am Thorac Soc*. 2008; 5:338–342. [PubMed: 18403330]
5. Osterreicher CH, Stickel F, Brenner DA. Genomics of liver fibrosis and cirrhosis. *Semin Liver Dis*. 2007; 27:28–43. [PubMed: 17295175]
6. Friedman SL. Mechanisms of hepatic fibrogenesis. *Gastroenterology*. 2008; 134:1655–1669. [PubMed: 18471545]
7. Karin M. Nuclear factor-kappaB in cancer development and progression. *Nature*. 2006; 441:431–436. [PubMed: 16724054]
8. De Minicis S, Bataller R, Brenner DA. NADPH oxidase in the liver: defensive, offensive, or fibrogenic? *Gastroenterology*. 2006; 131:272–275. [PubMed: 16831609]

9. Bataller R, Schwabe RF, Choi YH, Yang L, Paik YH, Lindquist J, Qian T, et al. NADPH oxidase signal transduces angiotensin II in hepatic stellate cells and is critical in hepatic fibrosis. *J Clin Invest.* 2003 Nov; 112(9):1383–1394. [PubMed: 14597764]
10. Laurent A, Nicco C, Chereau C, Goulvestre C, Alexandre J, Alves A, Levy E, et al. Controlling tumor growth by modulating endogenous production of reactive oxygen species. *Cancer Res.* 2005; 65:948–956. [PubMed: 15705895]
11. De Minicis S, Seki E, Uchinami H, Kluwe J, Zhang Y, Brenner DA, Schwabe RF. Gene expression profiles during hepatic stellate cell activation in culture and in vivo. *Gastroenterology.* 2007; 132:1937–1946. [PubMed: 17484886]
12. Urtasun R, Conde de la Rosa L, Nieto N. Oxidative and nitrosative stress and fibrogenic response. *Clin Liver Dis.* 2008; 12:769–790. viii. [PubMed: 18984466]
13. El-Benna J, Dang PM, Gougerot-Pocidallo MA, Marie JC, Braut-Boucher F. p47phox, the phagocyte NADPH oxidase/NOX2 organizer: structure, phosphorylation and implication in diseases. *Exp Mol Med.* 2009; 41:217–225. [PubMed: 19372727]
14. Dale DC, Boxer L, Liles WC. The phagocytes: neutrophils and monocytes. *Blood.* 2008; 112:935–945. [PubMed: 18684880]
15. Thakur V, McMullen MR, Pritchard MT, Nagy LE. Regulation of macrophage activation in alcoholic liver disease. *J Gastroenterol Hepatol.* 2007; 22 (Suppl 1):S53–56. [PubMed: 17567466]
16. Babior BM, Lambeth JD, Nauseef W. The neutrophil NADPH oxidase. *Arch Biochem Biophys.* 2002; 397:342–344. [PubMed: 11795892]
17. Zhan SS, Jiang JX, Wu J, Halsted C, Friedman SL, Zern MA, Torok NJ. Phagocytosis of apoptotic bodies by hepatic stellate cells induces NADPH oxidase and is associated with liver fibrosis in vivo. *Hepatology.* 2006; 43:435–443. [PubMed: 16496318]
18. De Minicis S, Seki E, Oesterreicher C, Schnabl B, Schwabe RF, Brenner DA. Reduced nicotinamide adenine dinucleotide phosphate oxidase mediates fibrotic and inflammatory effects of leptin on hepatic stellate cells. *Hepatology.* 2008; 48:2016–2026. [PubMed: 19025999]
19. Wheeler MD, Kono H, Yin M, Nakagami M, Uesugi T, Arteel GE, Gabele E, et al. The role of Kupffer cell oxidant production in early ethanol-induced liver disease. *Free Radic Biol Med.* 2001; 31:1544–1549. [PubMed: 11744328]
20. Adachi T, Togashi H, Suzuki A, Kasai S, Ito J, Sugahara K, Kawata S. NAD(P)H oxidase plays a crucial role in PDGF-induced proliferation of hepatic stellate cells. *Hepatology.* 2005; 41:1272–1281. [PubMed: 15915457]
21. Reinehr R, Becker S, Keitel V, Eberle A, Grether-Beck S, Haussinger D. Bile salt-induced apoptosis involves NADPH oxidase isoform activation. *Gastroenterology.* 2005; 129:2009–2031. [PubMed: 16344068]
22. Chang YC, Segal BH, Holland SM, Miller GF, Kwon-Chung KJ. Virulence of catalase-deficient *aspergillus nidulans* in p47(phox)^{-/-} mice. Implications for fungal pathogenicity and host defense in chronic granulomatous disease. *J Clin Invest.* 1998; 101:1843–1850. [PubMed: 9576747]
23. dela Pena A, Leclercq IA, Williams J, Farrell GC. NADPH oxidase is not an essential mediator of oxidative stress or liver injury in murine MCD diet-induced steatohepatitis. *J Hepatol.* 2007; 46:304–313. [PubMed: 17157947]
24. Kodama Y, Taura K, Miura K, Schnabl B, Osawa Y, Brenner DA. Antiapoptotic effect of c-Jun N-terminal Kinase-1 through Mcl-1 stabilization in TNF-induced hepatocyte apoptosis. *Gastroenterology.* 2009; 136:1423–1434. [PubMed: 19249395]
25. Seki E, De Minicis S, Oesterreicher CH, Kluwe J, Osawa Y, Brenner DA, Schwabe RF. TLR4 enhances TGF-beta signaling and hepatic fibrosis. *Nat Med.* 2007; 13:1324–1332. [PubMed: 17952090]
26. Kisseleva T, Uchinami H, Feirt N, Quintana-Bustamante O, Segovia JC, Schwabe RF, Brenner DA. Bone marrow-derived fibrocytes participate in pathogenesis of liver fibrosis. *J Hepatol.* 2006; 45:429–438. [PubMed: 16846660]
27. Van Rooijen N, Sanders A. Liposome mediated depletion of macrophages: mechanism of action, preparation of liposomes and applications. *J Immunol Methods.* 1994; 174:83–93. [PubMed: 8083541]
28. Babior BM. NADPH oxidase: an update. *Blood.* 1999; 93:1464–1476. [PubMed: 10029572]

29. Albano E. Alcohol, oxidative stress and free radical damage. *Proc Nutr Soc.* 2006; 65:278–290. [PubMed: 16923312]
30. Bedard K, Krause KH. The NOX family of ROS-generating NADPH oxidases: physiology and pathophysiology. *Physiol Rev.* 2007; 87:245–313. [PubMed: 17237347]
31. Bokoch GM, Zhao T. Regulation of the phagocyte NADPH oxidase by Rac GTPase. *Antioxid Redox Signal.* 2006; 8:1533–1548. [PubMed: 16987009]
32. Takeya R, Ueno N, Sumimoto H. Regulation of superoxide-producing NADPH oxidases in nonphagocytic cells. *Methods Enzymol.* 2006; 406:456–468. [PubMed: 16472678]
33. Canbay A, Taimr P, Torok N, Higuchi H, Friedman S, Gores GJ. Apoptotic body engulfment by a human stellate cell line is profibrogenic. *Lab Invest.* 2003; 83:655–663. [PubMed: 12746475]
34. Kono H, Rusyn I, Uesugi T, Yamashina S, Connor HD, Dikalova A, Mason RP, et al. Diphenyleioidonium sulfate, an NADPH oxidase inhibitor, prevents early alcohol-induced liver injury in the rat. *Am J Physiol Gastrointest Liver Physiol.* 2001; 280:G1005–1012. [PubMed: 11292610]
35. Tsukamoto H, Rippe R, Niemela O, Lin M. Roles of oxidative stress in activation of Kupffer and Ito cells in liver fibrogenesis. *J Gastroenterol Hepatol.* 1995; 10 (Suppl 1):S50–53. [PubMed: 8589343]
36. Kono H, Bradford BU, Rusyn I, Fujii H, Matsumoto Y, Yin M, Thurman RG. Development of an intragastric enteral model in the mouse: studies of alcohol-induced liver disease using knockout technology. *J Hepatobiliary Pancreat Surg.* 2000; 7:395–400. [PubMed: 11180860]
37. Baffy G. Kupffer cells in non-alcoholic fatty liver disease: the emerging view. *J Hepatol.* 2009; 51:212–223. [PubMed: 19447517]
38. Kono H, Rusyn I, Yin M, Gabele E, Yamashina S, Dikalova A, Kadiiska MB, et al. NADPH oxidase-derived free radicals are key oxidants in alcohol-induced liver disease. *J Clin Invest.* 2000; 106:867–872. [PubMed: 11018074]
39. Lambeth JD. Nox/Duox family of nicotinamide adenine dinucleotide (phosphate) oxidases. *Curr Opin Hematol.* 2002; 9:11–17. [PubMed: 11753072]
40. Mizrahi A, Molshanski-Mor S, Weinbaum C, Zheng Y, Hirshberg M, Pick E. Activation of the phagocyte NADPH oxidase by Rac Guanine nucleotide exchange factors in conjunction with ATP and nucleoside diphosphate kinase. *J Biol Chem.* 2005; 280:3802–3811. [PubMed: 15557278]
41. Siow YL, Au-Yeung KK, Woo CW, OK. Homocysteine stimulates phosphorylation of NADPH oxidase p47phox and p67phox subunits in monocytes via protein kinase C β activation. *Biochem J.* 2006; 398:73–82. [PubMed: 16626305]
42. Leto TL, Geiszt M. Role of Nox family NADPH oxidases in host defense. *Antioxid Redox Signal.* 2006; 8:1549–1561. [PubMed: 16987010]
43. van der Poorten D, Milner KL, Hui J, Hodge A, Trenell MI, Kench JG, London R, et al. Visceral fat: a key mediator of steatohepatitis in metabolic liver disease. *Hepatology.* 2008; 48:449–457. [PubMed: 18627003]
44. Cubero FJ, Nieto N. Ethanol and arachidonic acid synergize to activate Kupffer cells and modulate the fibrogenic response via tumor necrosis factor alpha, reduced glutathione, and transforming growth factor beta-dependent mechanisms. *Hepatology.* 2008; 48:2027–2039. [PubMed: 19003881]
45. De Minicis S, Brenner DA. Oxidative stress in alcoholic liver disease: role of NADPH oxidase complex. *J Gastroenterol Hepatol.* 2008; 23 (Suppl 1):S98–103. [PubMed: 18336675]
46. Korenaga M, Wang T, Li Y, Showalter LA, Chan T, Sun J, Weinman SA. Hepatitis C virus core protein inhibits mitochondrial electron transport and increases reactive oxygen species (ROS) production. *J Biol Chem.* 2005; 280:37481–37488. [PubMed: 16150732]
47. Wieckowska A, McCullough AJ, Feldstein AE. Noninvasive diagnosis and monitoring of nonalcoholic steatohepatitis: present and future. *Hepatology.* 2007; 46:582–589. [PubMed: 17661414]
48. Schattenberg JM, Wang Y, Rigoli RM, Koop DR, Czaja MJ. CYP2E1 overexpression alters hepatocyte death from menadione and fatty acids by activation of ERK1/2 signaling. *Hepatology.* 2004; 39:444–455. [PubMed: 14767997]

49. Minana JB, Gomez-Cambronero L, Lloret A, Pallardo FV, Del Olmo J, Escudero A, Rodrigo JM, et al. Mitochondrial oxidative stress and CD95 ligand: a dual mechanism for hepatocyte apoptosis in chronic alcoholism. *Hepatology*. 2002; 35:1205–1214. [PubMed: 11981771]

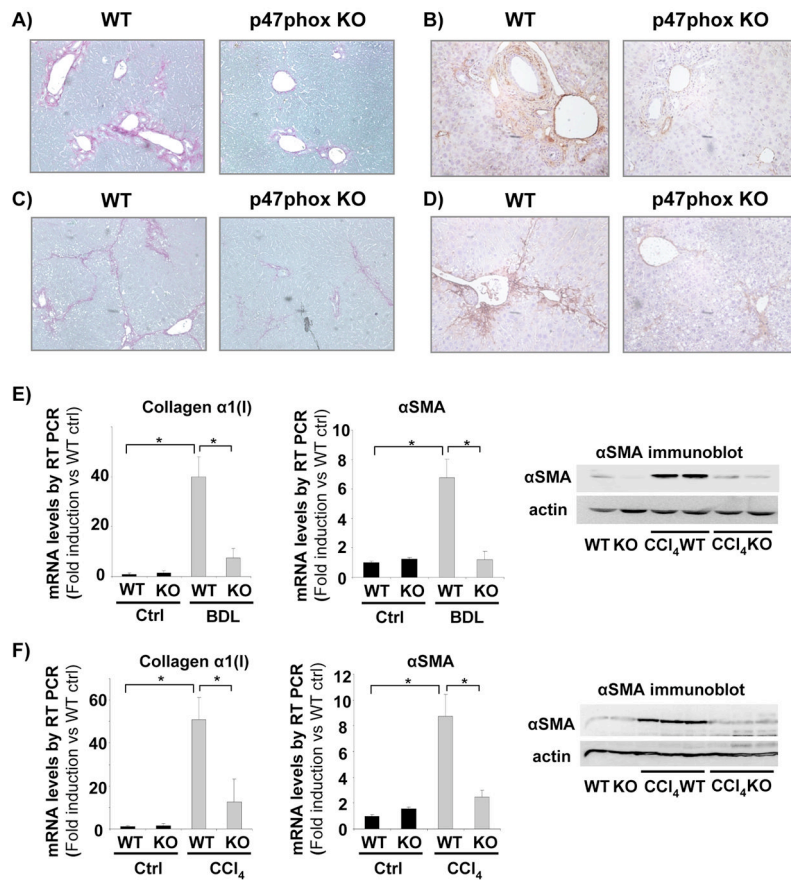


Figure 1. NOX deficient (p47^{phox} knock out (KO)) mice are resistant to liver fibrosis induced by bile duct ligation (BDL) or carbon tetrachloride (CCl₄)

(A, B) Sirius red staining of liver sections from WT and p47^{phox} KO mice 3 weeks after BDL or (C, D) after 16 injections (every 3 days) of CCl₄. (E, F) mRNA expression of Collagen α1(I) and αSMA were evaluated by quantitative real-time PCR from RNA extracted from total liver tissue of WT and p47^{phox} KO mice 3 weeks after BDL (E) or 16 injections of CCl₄ (F). Protein expression of αSMA was evaluated by western blot analysis from livers of wild type or p47^{phox} KO mice after 3 weeks of BDL (E) or 16 injections of CCl₄ (F). *, p < 0.05. Original Magnification, ×100 (A–D). Data are representative of three independent experiments.

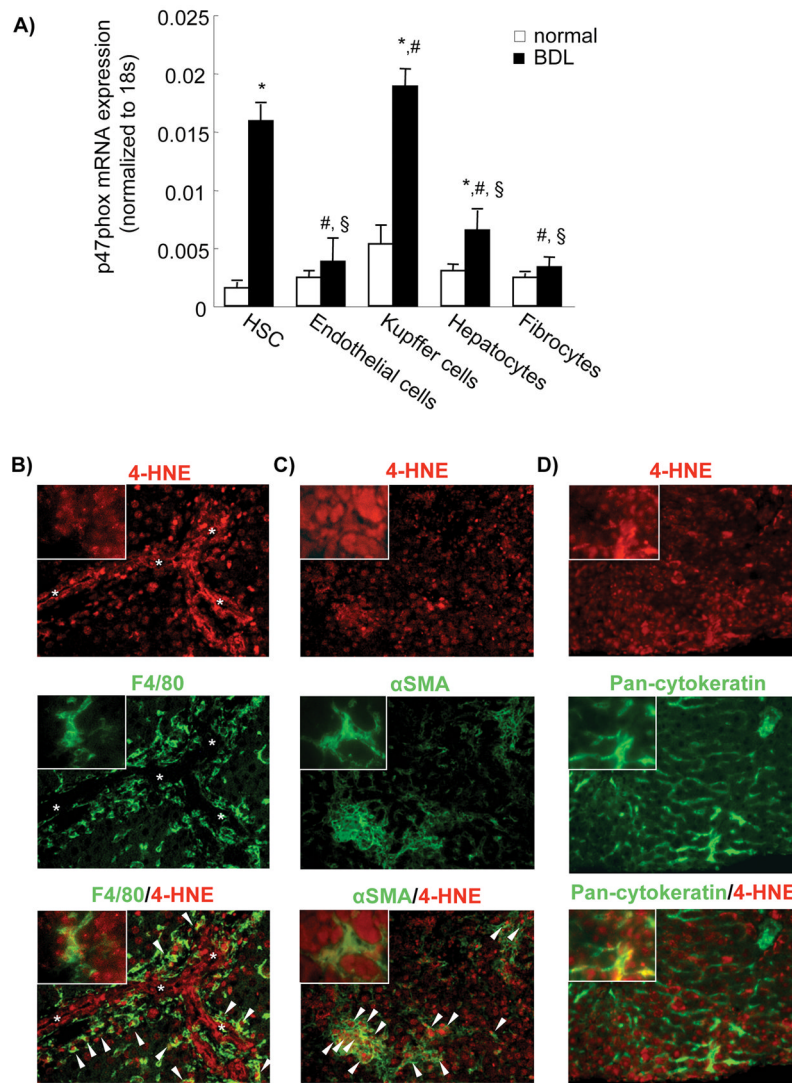


Figure 2. NOX expression and ROS production in different liver cell types

(A) mRNA expression of p47phox was evaluated by quantitative real-time PCR from RNA extracted from different cell types, including hepatic stellate cells (HSC), Endothelial cells, Kupffer cells, Hepatocytes and Fibrocytes, isolated from control mice or mice 2 weeks after bile duct ligation (n=3). *, p<0.05 cells isolated from BDL mice vs normal mice; #, p<0.05 cells isolated from BDL mice vs HSCs isolated from BDL mice; \$, p<0.05 cells isolated from BDL mice vs Kupffer cells isolated from BDL mice. (B–D) Double immunofluorescence staining for 4-hydroxynonenal (4-HNE) (red fluorescence, upper panel) and (B) F4/80 (KC), (C) αSMA (HSC) or (D) Pan-cytokeratin (HEP) (all green fluorescence, middle panel). The liver sections were from (B–D) bile duct-ligated mice. Arrow head indicates double positive cells. Asterisk indicates bile duct lumens. Original magnification, ×200 (B–D). Magnification of the inset, ×400 (B–D). Data are representative of three independent experiments.

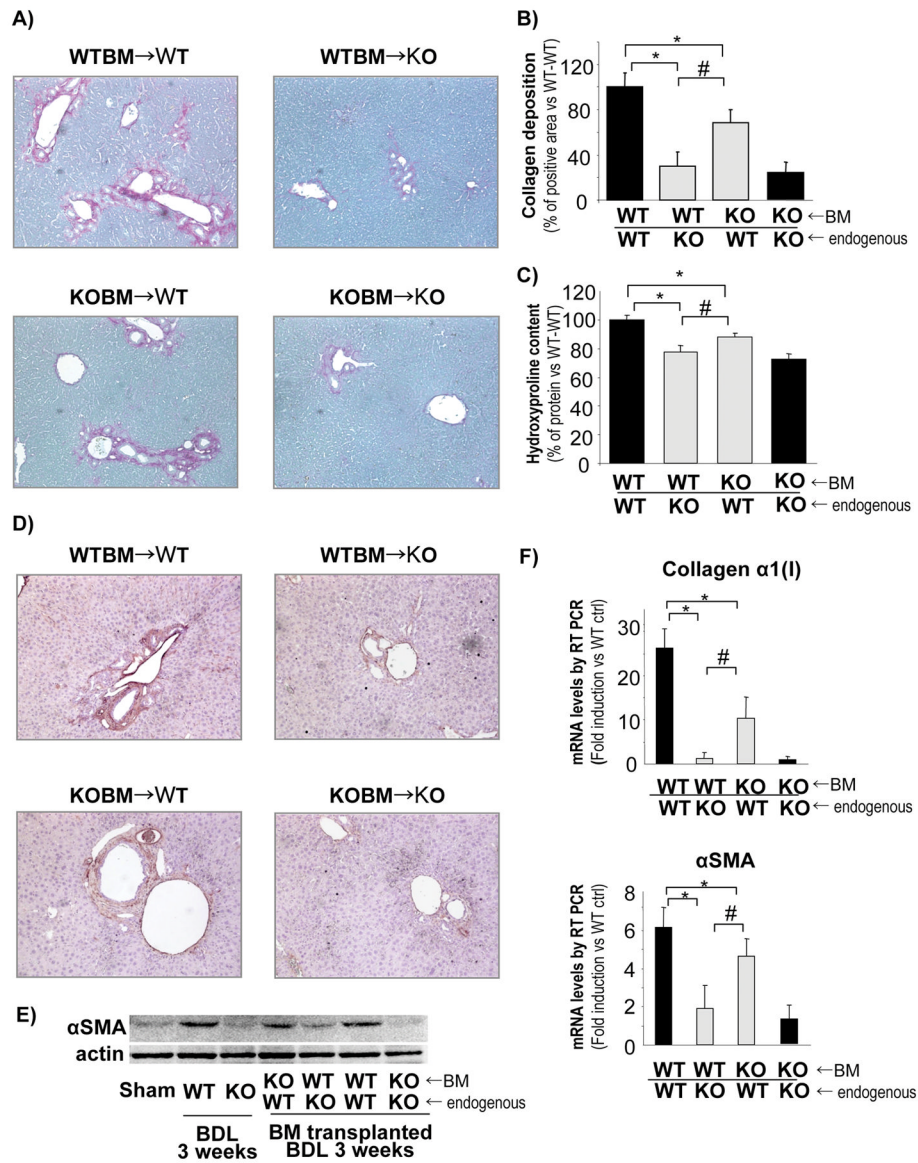


Figure 3. Chimeric mice with NOX-deficient (p47^{phox} KO) recipient cells have decreased fibrosis compared to mice with NOX-deficient bone marrow (BM)-derived cells
Chimeric mice were generated by injecting BM cells into mice pretreated with clodronate and lethal irradiation. The following groups were generated: WT BM → WT mice; WT BM → p47^{phox} KO mice; p47^{phox} KO BM → WT mice, and p47^{phox} KO BM → p47^{phox} KO mice. **(A)** Collagen deposition assessed by Sirius red staining, **(B)** Quantification of collagen deposition by computerized imaging analysis and **(C)** Hydroxyproline content assessed by absorbance assay, were evaluated in chimeric mice. *, $p < 0.05$ vs WT BM → WT mice; #, $p < 0.045$ vs p47^{phox} KO BM → WT mice. **(D)** Immunohistochemistry for αSMA. **(E)** Western blot from total liver samples for αSMA. **(F)** Quantification by qPCR of mRNA expression for collagen α1(I) and αSMA in all groups of chimeric mice. *, $p < 0.05$ vs WT BM → WT mice; #, $p < 0.045$ vs p47^{phox} KO BM → WT mice. Original Magnification, ×100 (A, D).

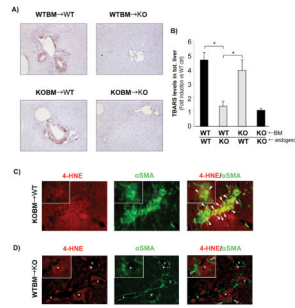


Figure 4. Chimeric mice with NOX-deficient (p47^{phox} KO) recipient cells have decreased peroxidation compared to mice with NOX-deficient BM-derived cells
(A) Immunohistochemistry for 4-hydroxynonenal (4-HNE) and **(B)** Thiobarbituric acid reactive substances (TBARS) measurement from total liver samples was evaluated in all groups of chimeric mice (as indicated in Fig. 3) after 3 weeks of BDL. *, p<0.05 vs WT BM → p47^{phox} KO mice. **(C, D)** Double immunofluorescence staining for 4-HNE (red fluorescence) and αSMA (green fluorescence) in **(C)** p47^{phox} KO BM → WT mice and **(D)** WT BM → p47^{phox} KO mice. Closed and open arrow heads indicate double positive cells and ROS negative cells, respectively. Asterisk indicates bile duct lumens. v, vessel lumens. Original Magnification, ×100 (A), ×200 (C, D). Magnification of the inset, ×400 (C, D).

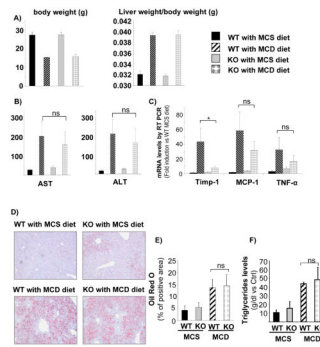


Figure 5. WT and NOX-deficient (p47^{phox} KO) mice fed with MCD diet for 10 weeks show comparable levels of steatosis and inflammation (A) body weight and liver weight/body weight ratio, (B) serum levels of AST and ALT and (C) mRNA levels of Timp-1, MCP-1 and TNF α in total liver samples were assessed in WT and KO mice treated with MCS and MCD diet for 10 weeks. *, $p < 0.05$ vs WT MCD. (D) Oil red O staining (E) and computerized quantification of lipid deposition, and (F) triglyceride content from total liver tissues were evaluated. Original Magnification, $\times 100$ (D),

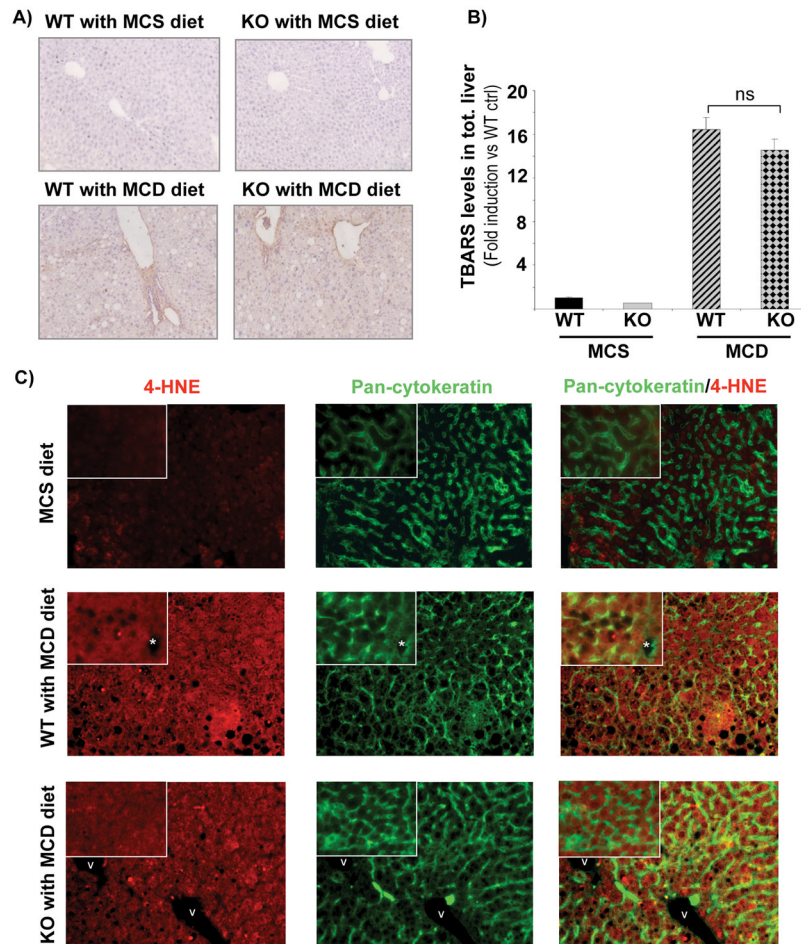


Figure 6. WT and NOX-deficient ($p47^{phox}$ KO) mice fed with MCD diet for 10 weeks show comparable levels of peroxidation (A) Immunohistochemistry for 4-hydroxynonenal (4-HNE) expression and (B) TBARS measurement from total liver tissues and (C) Double Immunofluorescence staining for 4-HNE (red fluorescence) and Pan-cytokeratin (parenchymal cell) (green fluorescence) was evaluated in wild type and $p47^{phox}$ KO mice fed for 10 weeks with an MCS or MCD diet. Asterisk indicates bile duct lumens. v, vessel lumens. Original Magnifications, $\times 100$ (A), $\times 200$ (C). Magnification of the inset, $\times 400$ (C).

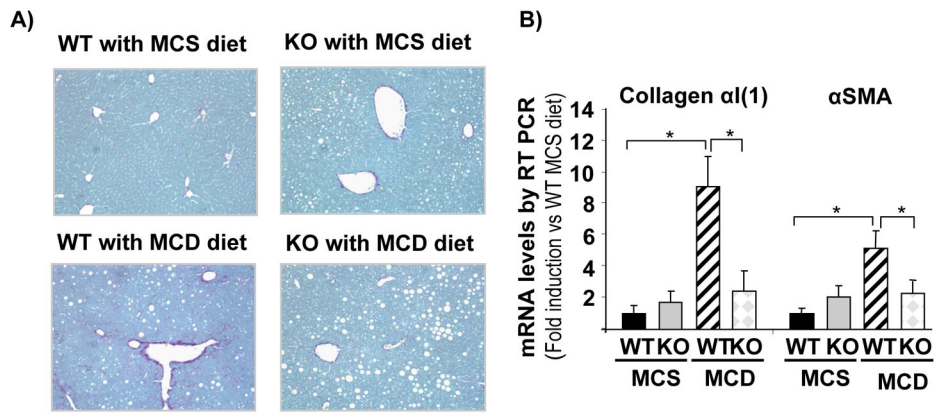


Figure 7. MCD diet for 10 weeks induced fibrosis in WT but not in NOX deficient (p47^{phox} KO) mice

(A) Sirius red staining of the livers of WT and p47^{phox} KO mice fed control MCS diet or MCD diet. (B) Quantitative real-time PCR of mRNA expressions for collagen α1(I) and αSMA in WT or p47^{phox} KO mice after 10 weeks of MCS or MCD diet are shown. *, p<0.05 vs WT MCD. Original Magnification, ×100 (A).

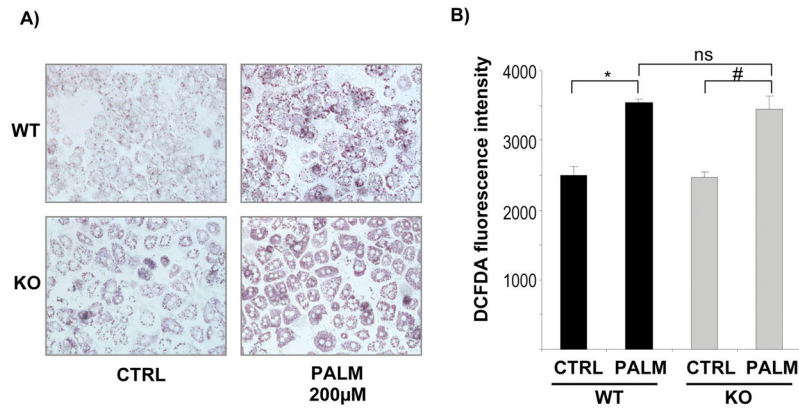


Figure 8. Both WT and NOX-deficient (p47^{phox} KO) hepatocytes treated with free fatty acids (FFAs) show increased lipid deposition and ROS production
Hepatocytes isolated from wild type and p47^{phox} KO mice were cultured on collagen I coated plastic dishes and incubated for 24 h with palmitic acid (PALM) (200 μM). **(A)** Lipid deposition was evaluated by Oil-Red O staining. **(B)** After 24 h incubation with PALM, hepatocytes were loaded with DCFDA (8 μM) for 20 minutes. Fluorescent signals were quantified using a fluorometer at excitation and emission wavelengths of 488 nm and 520 nm, respectively. *, p<0.05 vs WT PALM; # p<0.05 vs KO PALM. Original Magnification, ×200 (A).